© 2020. Published by The Company of Biologists Ltd | Development (2020) 147, dev187021. doi:10.1242/dev.187021

RESEARCH ARTICLE

Downregulation of the GHRH/GH/IGF1 axis in a mouse model of Börjeson-Forssman-Lehman syndrome

Helen M. McRae[1,2], Samantha Eccles[1], Lachlan Whitehead[1,2], Warren S. Alexander[1,2], Jozef Gécz[3], Tim Thomas[1,2,*,‡] and Anne K. Voss[1,2,*,‡]

ABSTRACT

Börjeson-Forssman-Lehmann syndrome (BFLS) is an intellectual disability and endocrine disorder caused by plant homeodomain finger 6 (*PHF6*) mutations. Individuals with BFLS present with short stature. We report a mouse model of BFLS, in which deletion of *Phf6* causes a proportional reduction in body size compared with control mice. Growth hormone (GH) levels were reduced in the absence of PHF6. *Phf6*$^{-/Y}$ animals displayed a reduction in the expression of the genes encoding GH-releasing hormone (GHRH) in the brain, GH in the pituitary gland and insulin-like growth factor 1 (IGF1) in the liver. *Phf6* deletion specifically in the nervous system caused a proportional growth defect, indicating a neuroendocrine contribution to the phenotype. Loss of suppressor of cytokine signaling 2 (SOCS2), a negative regulator of growth hormone signaling partially rescued body size, supporting a reversible deficiency in GH signaling. These results demonstrate that PHF6 regulates the GHRH/GH/IGF1 axis.

KEY WORDS: PHF6, Plant homeodomain finger protein 6, Börjeson-Forssman-Lehman Syndrome, BFLS, Failure to thrive, Growth hormone releasing hormone, Growth hormone, IGF-1, Insulin-like growth factor 1, SOCS2, Suppressor of cytokine signaling 2

INTRODUCTION

The Börjeson-Forssman-Lehmann syndrome (BFLS; OMIM 301900) is a rare intellectual disability syndrome caused by mutations in the X-linked gene *PHF6* (Börjeson et al., 1962; Lower et al., 2002). The disorder affects all known males with deleterious hemizygous *PHF6* mutations, while females heterozygous for *PHF6* mutations range from a full presentation of BFLS that is similar to males to apparently unaffected carriers (Berland et al., 2011; Crawford et al., 2006; Zweier et al., 2013). Neurological symptoms of BFLS include low IQ and susceptibility to seizures (Turner et al., 2004). Physical characteristics of BFLS in both males and females include deep-set eyes, large ears, tapering fingers and short toes (Turner et al., 2004). Several clinical signs of BFLS, including short stature, truncal obesity, gynecomastia and genital hypoplasia, point to disrupted endocrine control (Turner et al., 2004).

The PHF6 protein contains two plant homeodomain (PHD) zinc fingers (Lower et al., 2002), which are domains that occur in chromatin-associated proteins implicated in transcriptional regulation (Aasland et al., 1995). Mutations of *PHF6* in BFLS occur along the length of the gene, indicating a likely loss or reduced function mechanism in the pathogenesis. PHF6 localizes to the nucleus (Lower et al., 2002) and associates with histone proteins, including H3 (Soto-Feliciano et al., 2017), and histone variants, including H1.2, H2B.1, H2A.Z and H3.1 (Todd and Picketts, 2012). PHF6 has been implicated in transcriptional regulation through association with the PAF1 and NuRD complexes (Todd and Picketts, 2012). PHF6 has recently been reported to function in processes other than transcription, including in non-homologous end-joining (Warmerdam et al., 2020), and as an E3 ubiquitin ligase (Oh et al., 2020). In addition to germline mutations in BFLS, somatic *PHF6* mutations occur in human hematological malignancies, including T-cell acute lymphoblastic leukemia (Van Vlierberghe et al., 2010) and acute myeloid leukemia (Van Vlierberghe et al., 2011). PHF6 has recently been proven to be a tumor suppressor (McRae et al., 2019), in addition to regulating hematopoietic stem and progenitor cell function (Hsu et al., 2019; McRae et al., 2019; Miyagi et al., 2019; Wendorff et al., 2019).

A recent report characterized the neurological features of a mouse model of BFLS with a patient-specific mutation involving replacement of cysteine 99 in the first PHF6 PHD finger with phenylalanine (PHF6^{C99F}) (Cheng et al., 2018). These mice displayed reduced levels of PHF6 protein, evidence of deficits in contextual and social recognition memory, and increased seizure susceptibility in response to epilepsy-inducing drugs (Cheng et al., 2018). Mice with the PHF6^{C99F} mutation were reported to weigh less and to have reduced body length (Cheng et al., 2018), recapitulating the short stature observed in BFLS. The mechanisms underpinning this growth defect have not been investigated.

The hypothalamic-pituitary axis controls endocrine function in mammals. Transcription and secretion of the anterior pituitary hormones, growth hormone (GH), thyroid stimulating hormone (TSH), adrenocorticotrophic releasing hormone (ACTH), and the gonadotropins luteinizing hormone (LH) and follicle stimulating (FSH) are stimulated by their respective hypothalamic releasing hormones, including growth hormone-releasing hormone (GHRH), thyrotrophin-releasing hormone (TRH), corticotrophin-releasing hormone (CRH) and gonadotropin-releasing hormone (GnRH) (Chrousos et al., 2009; Ikegami and Yoshimura, 2017; Ranke and Wit, 2018; Stamatiades and Kaiser, 2018; Thackray et al., 2010), while prolactin (PRL) secretion is primarily controlled via negative regulation by dopamine (Bernard et al., 2019). The anterior pituitary hormones (GH, TSH, LH, FSH, ACTH and PRL) are secreted into the bloodstream and in turn regulate production of downstream hormones at peripheral sites. Pituitary hormones exert pleiotropic effects, including the control of growth in the case of the GH and thyroid axes (Ikegami and Yoshimura, 2017; Ranke and Wit, 2018).

[1]Walter and Eliza Hall Institute of Medical Research, Melbourne, Victoria 3052, Australia. [2]Department of Medical Biology, The University of Melbourne, Victoria 3052, Australia. [3]Adelaide Medical School and the Robinson Research Institute, The University of Adelaide, Adelaide, SA 5005, Australia.
*These authors contributed equally to this work and share senior authorship

‡Author for correspondence (avoss@wehi.edu.au; tthomas@wehi.edu.au)

J.G., 0000-0002-7884-6861; A.K.V., 0000-0002-3853-9381

Handling Editor: Sally Dunwoodie
Received 5 December 2019; Accepted 9 September 2020

Development (2020) 147, dev187021. doi:10.1242/dev.187021

Endocrine testing of individuals with BFLS has revealed alterations in pituitary hormone levels in some patients [see Table S1, adapted from a summary by Zhang et al. (2019)]. Specifically, GH was found to be lower than average in three out of four males (Birrell et al., 2003; Dereymaeker et al., 1986; Robinson et al., 1983) and three out of four females assayed (Petridou et al., 1997; Robinson et al., 1983; Zhang et al., 2019). TSH was decreased in two out of four assessed males (Birrell et al., 2003; Dereymaeker et al., 1986; Robinson et al., 1983; Turner et al., 1989; Weber et al., 1978) and increased in one out of five assessed females (Birrell et al., 2003; Carter et al., 2009; Crawford et al., 2006; Matsuo et al., 1984; Petridou et al., 1997; Robinson et al., 1983; Zhang et al., 2019). As both the GH and thyroid axis control growth (Wit et al., 2016), it is possible the reduced function of one or both of these pathways is responsible for the observed short stature in BFLS.

PRL levels were reported to be unchanged in one male tested (Robinson et al., 1983) and in three females tested (Petridou et al., 1997; Robinson et al., 1983), while ACTH deficiency was mentioned in a case report of two brothers (Birrell et al., 2003). Testosterone levels were commonly affected, with 11 out of 14 males showing a decrease (Ardinger et al., 1984; Baumstark et al., 2003; Carter et al., 2009; de Winter et al., 2009; Robinson et al., 1983; Turner et al., 1989; Weber et al., 1978). Levels of the gonadotropins LH and FSH were raised in some cases but lowered in others (Table S1), leading to the hypothesis that BFLS may involve both central and peripheral defects of the gonadotropin axis (Robinson et al., 1983).

It is important to note that these endocrine tests have been performed in various laboratories over a span of more than 40 years. Consequently, it is unclear whether the discrepancy in results represents true variation between individuals (perhaps due to different genetic variants in the *PHF6* gene, polymorphisms in the genetic background and/or environmental factors), variable testing procedures or other factors, such as the age at which patients were tested.

Although the endocrine test results are variable among individuals with BFLS, the symptoms of BFLS, including frequent short stature (with a normal birth weight), small genitalia and gynecomastia (Gécz et al., 2006), along with altered pituitary hormone levels identified in a number of BFLS patients led us to hypothesize that loss of PHF6 may disrupt hypothalamic-pituitary axis function. Therefore, we sought to characterize the role of PHF6 in regulation of this axis. Here, we report the phenotype of a novel mouse model of BFLS and identify PHF6 as a key regulator of the GHRH/GH/IGF1 axis, which controls growth, at least in part, through regulation within the nervous system.

RESULTS

Mice lacking PHF6 survive on the FVB/BALB/C background and display a postnatal growth defect

To study the role of PHF6 in the endocrine system, we used a murine *Phf6* allele with *loxP* sites flanking exon 4 and 5 (McRae et al., 2019), which results in undetectable *Phf6* mRNA upon cre-mediated recombination (Fig. S1A). As previously reported, males with germline deletion of *Phf6* on a C57BL/6 background died shortly after birth, while heterozygous females survive to adulthood (McRae et al., 2019). Female mice with germline mutation in one copy of *Phf6* had a significantly reduced body weight compared with control mice (P<0.001; Fig. 1A). A significant difference was detected by 3 weeks of age using Bonferroni's post-hoc test for multiple comparisons (7.47±0.33 g versus 9.00±0.25 g for $Phf6^{+/-}$ and $Phf6^{+/+}$ mice, respectively, P=0.01; Fig. 1A). Male $Phf6^{-/Y}$ mice isolated just before birth at E18.5 had an equal body weight compared with controls (1.13±0.04 g versus 1.13±0.05 g, P=0.96; Fig. S1B), indicating the effect of PHF6 on growth and survival occurs postnatally.

The survival of human BFLS patients with mutations expected to result in complete loss of PHF6 suggest that hemizygous *PHF6* loss-of-function mutations should be compatible with postnatal life. We hypothesized that the genetic background may be an important determinant of survival. In order to model an outbred genetic background that may more closely represent the effect of loss-of-function mutations in humans, we bred the $Phf6^{-}$ allele onto a mixed FVB/BALB/c background. In contrast to the C57BL/6 background, $Phf6^{-/Y}$ males survived postnatally on the mixed FVB/BALB/c background, although they were slightly underrepresented by weaning with 17.7% versus the expected 25% (P=0.0498; Table S2), for reasons yet to be determined. Once weekly weighing showed that adult $Phf6^{-/Y}$ mice have a reduction in body weight compared with wild-type mice (P<0.001), with a significant difference detected by 2 weeks of age with Bonferroni's post-hoc test for multiple comparisons (5.13±0.45 g, versus 8.27±0.39 g, P<0.001; Fig. 1B). The largest difference in body weight was at 3 weeks of age where *Phf6*-deleted mice were ∼50% smaller than controls (5.40±0.66 versus 10.72±0.47, P<0.001; Fig. 1B). Body length (79.75±2.02 mm versus 96.00±1.08 mm) and femur length (9.75±0.32 mm versus 11.75±0.14 mm) was significantly reduced in $Phf6^{-/Y}$ mice compared with controls (P=0.0004 and 0.001, respectively; Fig. 1C-E), indicating the reduced body weight is a result of reduced overall growth rather than reduced adipose tissue. Indeed, relative to body weight, $Phf6^{-/Y}$ mice had an increase in the inguinal subcutaneous and dorsal lumbar white fat compared with controls (0.019±0.002 g versus 0.011±0.001 g, respectively, P=0.02), but no change in the interscapular brown adipose tissue (Fig. 1F). In absolute terms, the lean body volume, but not the adipose tissue volume, was significantly reduced in the $Phf6^{-/Y}$ mice compared with controls (Fig. 1G). Males of the $Phf6^{-/Y}$ genotype were fertile. Intercrosses between $Phf6^{-/Y}$ and $Phf6^{-/+}$ demonstrated that FVB/BALB/c females with homozygous mutation in *Phf6* could survive and, as was demonstrated for $Phf6^{-/+}$ heterozygous females, they were smaller than control females (10.41±0.80 g, 8.32±0.33 g and 7.00±0.01 g for $Phf6^{+/+}$, $Phf6^{-/+}$ and $Phf6^{-/-}$ genotypes, respectively, at 3 weeks of age; P=0.01 for $Phf6^{-/-}$ versus $Phf6^{+/+}$ and P=0.02 for $Phf6^{-/+}$ versus $Phf6^{+/+}$; Fig. S1C).

Phf6 deletion results in reduced GH secretion and reduced pituitary gland GH levels

To test whether the loss of PHF6 altered circulating levels of pituitary hormones, we assayed the concentrations of ACTH, GH, FSH, LH, PRL and TSH using a multiplex assay in male mice on the FVB/BALB/c background. Because of the pulsatile nature of pituitary hormone secretion (Steyn et al., 2011, 2013), we assayed blood isolated every 10 min over 6 h (Fig. 2A, Fig. S2).

Given the smaller size of the $Phf6^{-/Y}$ animals, we hypothesized that there would be lower levels of GH. As expected, $Phf6^{-/Y}$ mice displayed a reduction in the mean concentration and total secreted GH (area under the curve) to 55% of control mice (Fig. 2A, Table 1). Deconvolution analysis using the AutoDecon algorithm (Johnson et al., 2008, 2009) indicated that the basal secretion rate of GH and the number of peaks were unaffected by PHF6, but there was a decrease in the maximum peak mass to 14% of controls and a decrease in the average peak mass in $Phf6^{-/Y}$ animals to 15% of $Phf6^{+/Y}$ littermates (Table 1).

Development (2020) 147, dev187021. doi:10.1242/dev.187021

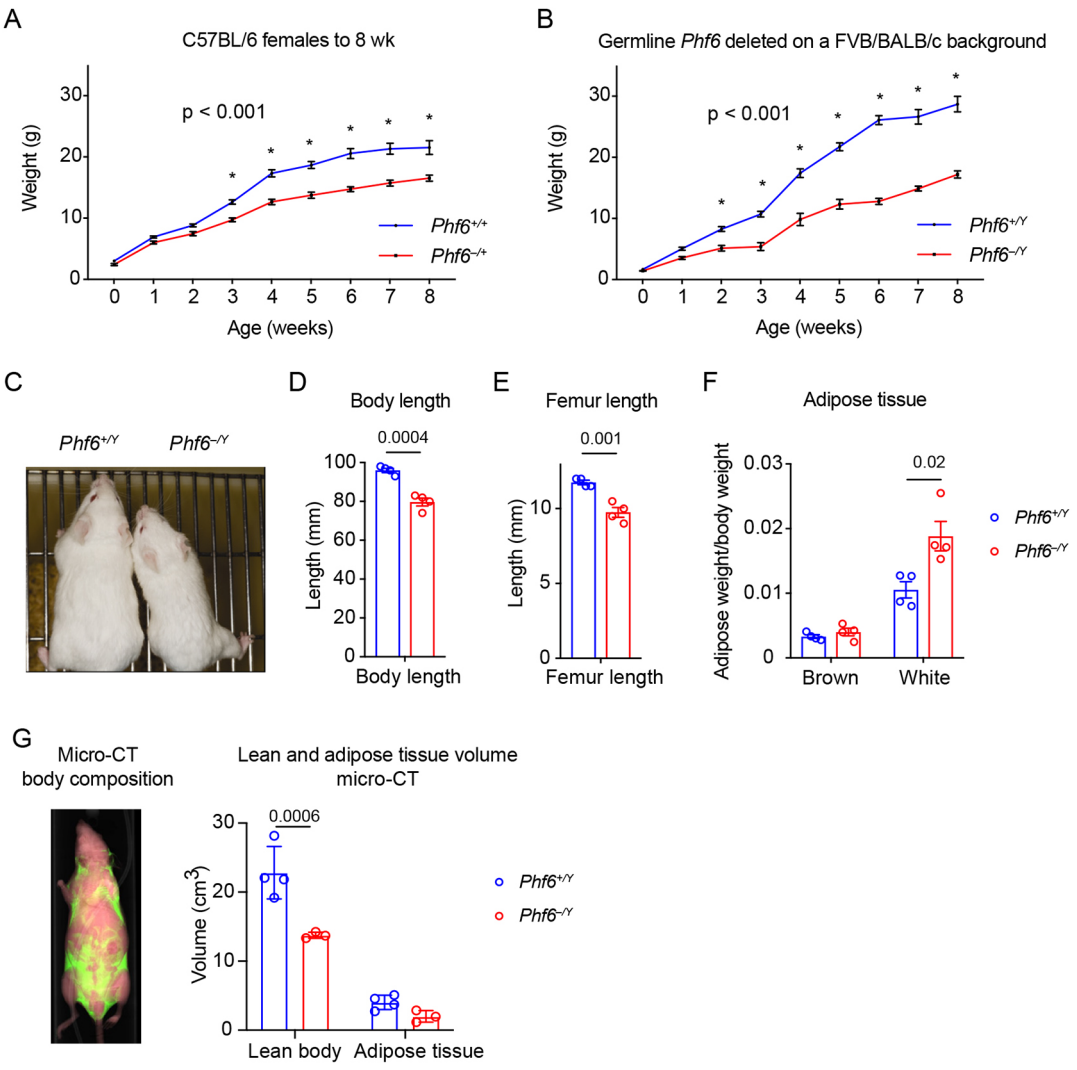

Fig. 1. Germline *Phf6* deletion causes a postnatal growth defect. (A) Heterozygous germline deletion of *Phf6* in females results in reduced overall body weight (C57BL/6 background). *n*=7 to 11 animals for each time point. (B) Hemizygous germline deletion of *Phf6* in males results in reduced overall body weight (FVB/BALB/c background). *n*=4 to 16 animals for each time point. (C) Representatives of *Phf6*$^{+/Y}$ (left) and *Phf6*$^{-/Y}$ (right) mice on the FVB/BALB/c background. (D) Body length is significantly reduced in *Phf6*$^{-/Y}$ compared with *Phf6*$^{+/Y}$ FVB/BALB/c mice. (E) Femur length is significantly reduced in *Phf6*$^{-/Y}$ compared with *Phf6*$^{+/Y}$ FVB/BALB/c mice. (F) Brown adipose tissue was isolated from the interscapular region, while white adipose tissue is pooled from the inguinal and dorsal lumbar regions for measurement. (G) Representative micro-CT image of a wild-type mouse and numerical assessment of the lean body volume and the adipose tissue volume by micro-CT in *Phf6*$^{-/Y}$ compared with *Phf6*$^{+/Y}$ FVB/BALB/c mice. *n*=3 to 4 animals per genotype and were 8-9 weeks old FVB/BALB/c mice (D-F). Data are mean±s.e.m. and were analyzed by a two-way ANOVA followed by Bonferroni's post-hoc test for multiple comparisons in A,B. The *P*-value in A,B indicates results of the overall effect of genotype in the two-way ANOVA analysis, while the asterisks indicate a $P<0.05$ in multiple comparison tests. Data points in D-G represent results of individual animals. Data in D-G were analyzed using an unpaired two-tailed Student's *t*-test.

To test whether the reduction in secreted GH levels corresponded to a reduction in pituitary GH levels, we performed western blots for GH using pituitary lysates and observed a reduction in GH protein, relative to the actin loading control, in *Phf6*$^{-/Y}$ pituitaries versus *Phf6*$^{+/Y}$ controls (Fig. 2B,C). These results indicate that pituitary GH and secreted GH levels are decreased in mice lacking PHF6.

Effect of PHF6 on other hypothalamic-pituitary axis pathways

In contrast to the effect of PHF6 on GH secretion, there was no effect of PHF6 loss on the concentration or secretion parameters of the other pituitary-derived hormones assessed: ACTH, FSH, LH, PRL and TSH (Fig. S2, Tables S3 to S7). Despite no change in the circulating levels of ACTH, FSH, LH, PRL and TSH between *Phf6*$^{-/Y}$ and control mice, we identified changes in the mRNA levels in hypothalamic pituitary axis genes of some of these pathways through assessing a panel of candidate genes by RT-qPCR. In male FVB/BALB/c *Phf6*$^{-/Y}$ mice, we found reduced mRNA levels of the prolactin gene *Prl* in the pituitary gland (Fig. S3A). Levels in the pituitary gland of the pro-opiomelanocortin gene *Pomc*, which encodes the ACTH precursor, were significantly reduced in *Phf6*$^{-/Y}$ versus control adult mice, whereas mRNA levels of corticotrophin-releasing hormone (*Crh*), which encodes the *Pomc* stimulating factor, were unchanged in the brain (Fig. S3B,C). Pituitary transcript levels of the gene encoding the common alpha subunit (*Cga*) for TSH, FSH and LH, the thyrotropin-releasing hormone β-subunit (*Tshb*), and the gonadotropin β-subunits (*Fshb* and *Lhb*), were not affected by *Phf6* status (Fig. S3D-G). *Trh* mRNA levels were unaffected in the adult brain (Fig. S3H); however, gonadotropin releasing hormone (*Gnrh1*) transcript levels were slightly reduced in the brain of adult *Phf6*$^{-/Y}$ versus control mice

Development (2020) 147, dev187021. doi:10.1242/dev.187021

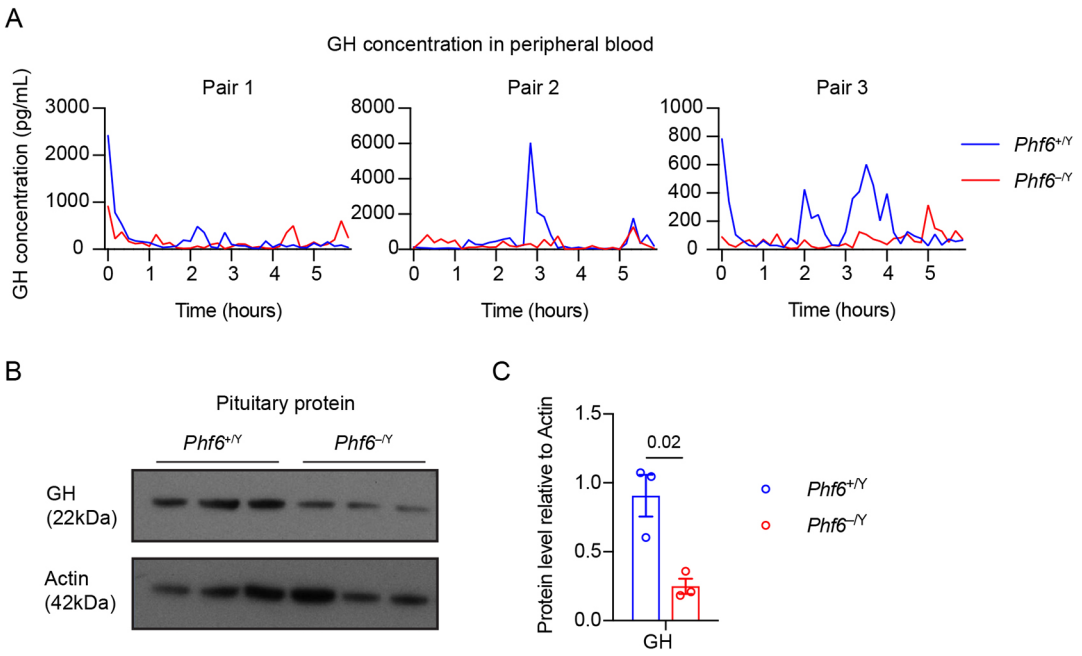

Fig. 2. Circulating and pituitary GH levels are reduced in *Phf6*$^{-/Y}$ mice. (A) GH concentration measured at 10 min intervals over a 6 h time period. Analysis of data is presented in Table 1. Each line displays data from one animal (*n*=3 animals per genotype). (B) Western blot showing GH and actin protein levels in pituitary lysates from *Phf6*$^{-/Y}$ and *Phf6*$^{+/Y}$ mice. Each lane represents protein from an individual animal (*n*=3 per genotype). (C) Quantification of data shown in B demonstrating reduced GH protein levels relative to actin protein in the pituitary of *Phf6*$^{-/Y}$ compared with *Phf6*$^{+/Y}$ mice. All data in this figure refer to mice on the FVB/BALB/c background. In C, the result from each individual animal is presented as a circle and mean±s.e.m. are shown. Data were analyzed using an unpaired two-tailed Student's *t*-test.

(Fig. S3I). These results indicate some evidence of a minor effect of PHF6 on the central hypothalamic-pituitary-gonadal axis in the form of an effect on brain *Gnrh1* mRNA levels, in addition to reduced pituitary gland transcript levels of *Prl* and *Pomc* caused by loss of PHF6. However, these changes at the mRNA level did not manifest as corresponding changes to the circulating levels of gonadotropins, PRL or ACTH proteins in FVB/BALB/c mice.

Deletion of *Phf6* results in reduced mRNA levels of GHRH/GH/IGF1 axis genes

Assessment of transcript levels of endocrine genes in the GH pathway in mice on the FVB/BALB/c background demonstrated a significant reduction in mRNA levels of the growth hormone-releasing hormone gene (*Ghrh*) in the brain of adult mice lacking PHF6 (Fig. 3A). On the other hand, loss of PHF6 had no effect on the expression of somatostatin (*Sst*), a negative regulator of GH release and secretion (Fig. 3B). In concordance with the reduced GH pituitary protein levels, transcripts of the growth hormone gene, *Gh*, in the pituitary gland were also significantly reduced both at postnatal day 14 (P14) and in adults (Fig. 3C). Transcript levels of the downstream effector gene of GH, *Igf1*, were reduced in the liver at P14 and in older mice in the absence of PHF6 (*Phf6*$^{-/Y}$) compared with controls (Fig. 3D). The absence of PHF6 (*Phf6*$^{-/Y}$) also resulted in a reduction in plasma IGF1 protein levels (Fig. 3E). These results indicate that downregulation of the GHRH/GH/IGF1 axis is likely to be responsible for the observed growth defect resulting from loss of PHF6.

Nervous system-specific deletion of *Phf6* results in a postnatal growth defect

The effect of PHF6 on transcription of GHRH/GH/IGF1 axis genes in the brain, pituitary gland and liver suggests that PHF6 could be playing a role in multiple tissues and at multiple levels of the GHRH/GH/IGF1 axis. To assess whether a neuroendocrine role of

Table 1. GH secretion parameters

	GH secretion analysis*						
Experimental group	Pair 1		Pair 2		Pair 3		
Genotype	*Phf6*$^{+/Y}$	*Phf6*$^{-/Y}$	*Phf6*$^{+/Y}$	*Phf6*$^{-/Y}$	*Phf6*$^{+/Y}$	*Phf6*$^{-/Y}$	*P*-value
Area under curve	80,454	58,245	1.92×10^5	1.01×10^5	59,739	23,094	0.04
Average concentration (pg/ml)	223.48	161.79	532.18	288.24	165.94	64.15	0.04
Basal secretion rate (pg/ml per min)	24.94	4.37	8.21	2.69×10^4	2.99	1.24	0.14
Number of peaks	3	4	7	1	6	4	0.20
Sum peak mass (pg)	13,791.3	3212.3	3.60×10^4	517.38	3501.16	817.51	0.06
Maximum peak mass (pg)	8955.9	1415.6	6144.9	517.38	1304.9	398.69	0.02
Average peak mass (pg)	4597.1	803.08	5143.79	517.38	583.53	204.38	0.02

*Analysis of data displayed in Fig. 2A. Secretion parameters were calculated using AutoDecon. *P*-value was determined using a one-tailed paired *t*-test for each parameter. The area under the curve, the average concentration, the maximum peak mass and the average peak mass were significantly reduced in *Phf6*$^{-/Y}$ compared with *Phf6*$^{+/Y}$ mice.

Development (2020) 147, dev187021. doi:10.1242/dev.187021

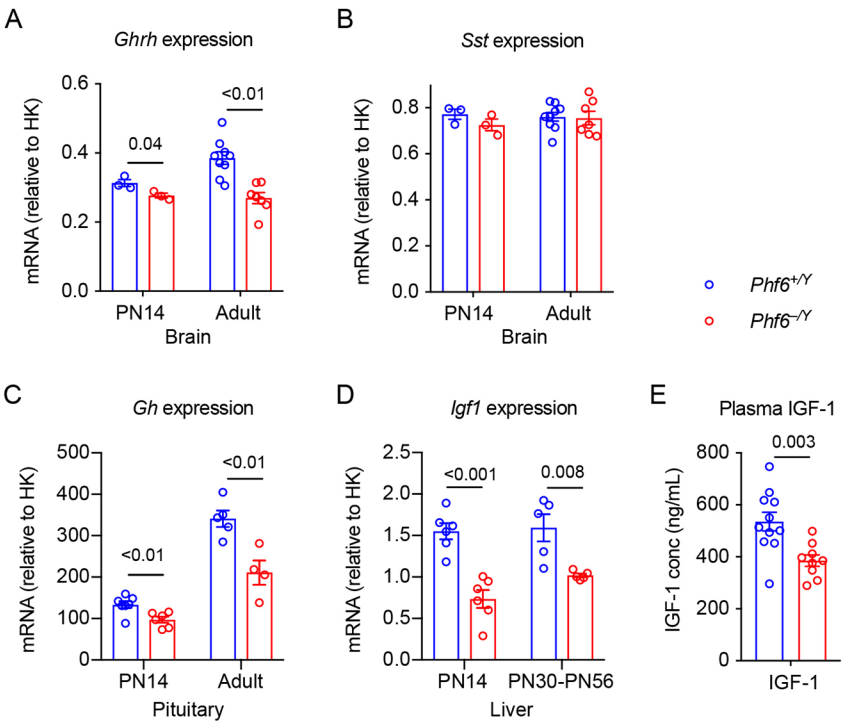

Fig. 3. mRNA levels of brain *Sst*, brain *Ghrh*, pituitary *Gh* and liver *Igf1* in *Phf6*$^{-/Y}$ mice compared with controls. RT-qPCR data are shown. (A) *Ghrh* mRNA levels in the brain of P14 and adult mice. (B) *Sst* mRNA levels in the brain of P14 and adult mice. (C) *Gh* mRNA levels in pituitaries isolated from P14 and adult mice. (D) *Igf1* mRNA levels in the liver of P14 and P30-P56 mice. (E) IGF1 protein levels in plasma as assessed by ELISA. Data are mean±s.e.m. of arbitrary units corresponding to the Cp values and are normalized to housekeeping (HK) genes (*Gapdh* and *Pgk1*). Each individual data point represents the result from one animal. Final mRNA values were analyzed using an unpaired two-tailed Student's *t*-test.

PHF6 was contributing to the growth defect, we employed the *Nestin-cre* transgene, which is expressed in the nervous system, including the hypothalamus, but not in the pituitary gland or the liver (Tronche et al., 1999). By crossing *Phf6* (*Phf6*^{lox}) mice with mice expressing the *Nestin-cre* transgene (*Nes-cre*$^{Tg/+}$), we deleted *Phf6* specifically in the nervous system on the C57BL/6 background (Fig. S4A,B). Males with nervous system deletion of *Phf6* (*Phf6*$^{lox/Y}$;*Nes-cre*$^{Tg/+}$) survived postnatally on the C57BL/6 background, indicating the perinatal death observed in C57BL/6 *Phf6*$^{-/Y}$ mice was not due to nervous system-specific effects. As the *Nestin-cre* transgene alone causes a mild postnatal growth defect (Declercq et al., 2015; Galichet et al., 2010), evident by 4 weeks of age (Fig. S4C), we compared *Phf6*$^{lox/Y}$;*Nes-cre*$^{Tg/+}$ mice with *Nes-cre*$^{Tg/+}$ controls to measure the effect of *Phf6*-deletion specifically. *Phf6*$^{lox/Y}$;*Nes-cre*$^{Tg/+}$ mice displayed a reduction in body weight compared with *Phf6*$^{+/Y}$;*Nes-cre*$^{Tg/+}$, with a statistically significant difference in multiple comparisons evident by postnatal week 3 (9.06±0.52 versus 5.13±0.30, respectively), corresponding to a 43% reduction in body weight (P<0.001; Fig. 4A). This effect was proportional, affecting overall body size (Fig. S4D). The effects of nervous system-specific deletion of *Phf6* were accompanied by a reduction in *Igf1* mRNA in the *Phf6*$^{lox/Y}$;*Nes-cre*$^{Tg/+}$ liver compared with controls (Fig. 4B). The effects of nervous system-specific deletion of *Phf6* on overall body growth and peripheral organs demonstrate that control of body growth by PHF6 is at least in part mediated by neuroendocrine signaling.

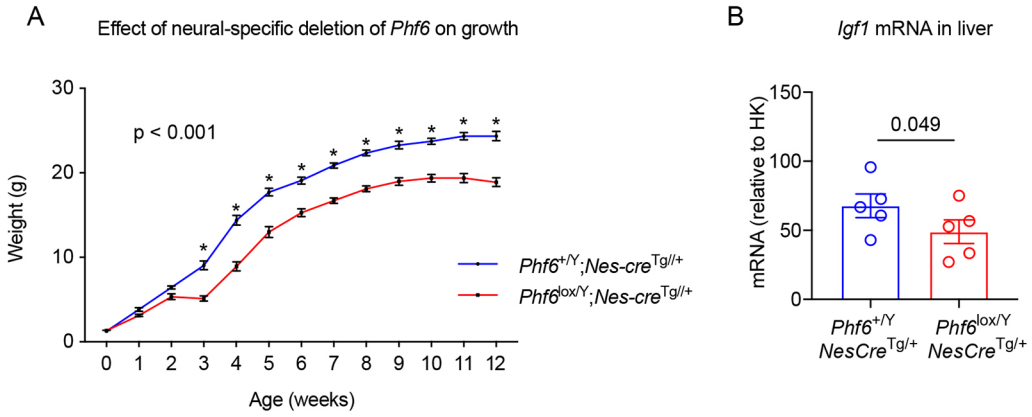

Fig. 4. Nervous system-specific deletion of *Phf6* causes a postnatal growth defect and a reduction in liver *Igf1* mRNA. (A) Weekly weight of control mice (*Phf6*$^{+/Y}$;*Nes-cre*$^{Tg/+}$, n=5 to 18 per time point) and mice with *Phf6* deleted in the nervous system (*Phf6*^{loxY};*Nes-cre*$^{Tg/+}$, n=4 to 14 per time point). Data are mean±s.e.m. and, were analyzed using a two-way ANOVA with genotype and age as the two independent factors and with Bonferroni's post-hoc test for comparisons at each time point. *P<0.05 for multiple comparison at that time point. (B) *Igf1* mRNA levels relative to the housekeeping (HK) gene *Gapdh*, assessed by RT-qPCR in the livers of 8- to 12-week-old *Phf6*^{loxY};*Nes-cre*$^{Tg/+}$ and *Phf6*$^{+/Y}$;*Nes-cre*$^{Tg/+}$ control mice. Data are mean±s.e.m. and were analyzed using an unpaired one-tailed Student's *t*-test. Each data point represents the result from one animal, n=5 animals per genotype.

Development (2020) 147, dev187021. doi:10.1242/dev.187021

Anterior pituitary gland cells produce a reduced amount of growth hormone

A reduction in anterior pituitary hormone protein in the pituitary gland in the absence of PHF6 (see GH in Fig. 2B,C) could result from a reduction in the number of hormone producing cells as a result of a defect in pituitary development or from a reduction in the amount of hormone produced per cell. To distinguish these two possibilities, we assessed the histology of the pituitary and GH, PRL, ACTH, TSH and FSH levels per cell by immunofluorescence in sections of *Phf6*$^{+/Y}$ and *Phf6*$^{-/Y}$ pituitary glands (Fig. 5, Fig. S5). The pituitary gland displayed a normal histological structure (Fig. 5A), but was smaller in *Phf6*$^{-/Y}$ mice compared to controls (not shown). Likewise, the volume of the anterior lobe specifically was smaller in *Phf6*$^{-/Y}$ mice than in control mice (Fig. 5B). However, the decrease in volume was proportional to the decrease in total body volume (Fig. 5C). The absence of PHF6 caused a reduction in GH immunofluorescence signal per cell and per animal (Fig. 5D-F), but not in the total cell number or the GH^{+} area per view field. Similarly, the PRL signal was reduced per cell *Phf6*$^{-/Y}$ mice compared with controls, but not the PRL^{+} area (Fig. S5A). Only ACTH, in addition to being reduced per cell, appeared to be present in a smaller area of the tissue in *Phf6*$^{-/Y}$ mice compared with controls (Fig. S5B). No significant differences were observed in TSH or FSH staining (Fig. S5C,D). These results suggest that PHF6 is required either directly or indirectly for the production of normal levels of GH, PRL and ACTH per cell, and possibly also for the development or survival of normal numbers of ACTH-producing cells.

The growth defect caused by loss of PHF6 is reversible by abolishing the negative regulation of GH signaling by the suppressor of cytokine signaling 2

Suppressor of cytokine signaling (SOCS) proteins provide important negative-feedback mechanisms for many signaling pathways. SOCS proteins act by binding to and blocking activation of phosphorylation sites and by serving as E3 ubiquitin ligase adapter proteins, committing signal cascade proteins to proteasomal degradation (Linossi et al., 2013; Rico-Bautista et al., 2006). SOCS2 is an important negative regulator of growth hormone receptor (GHR) signaling and, as such, *Socs2*$^{-/-}$ mice

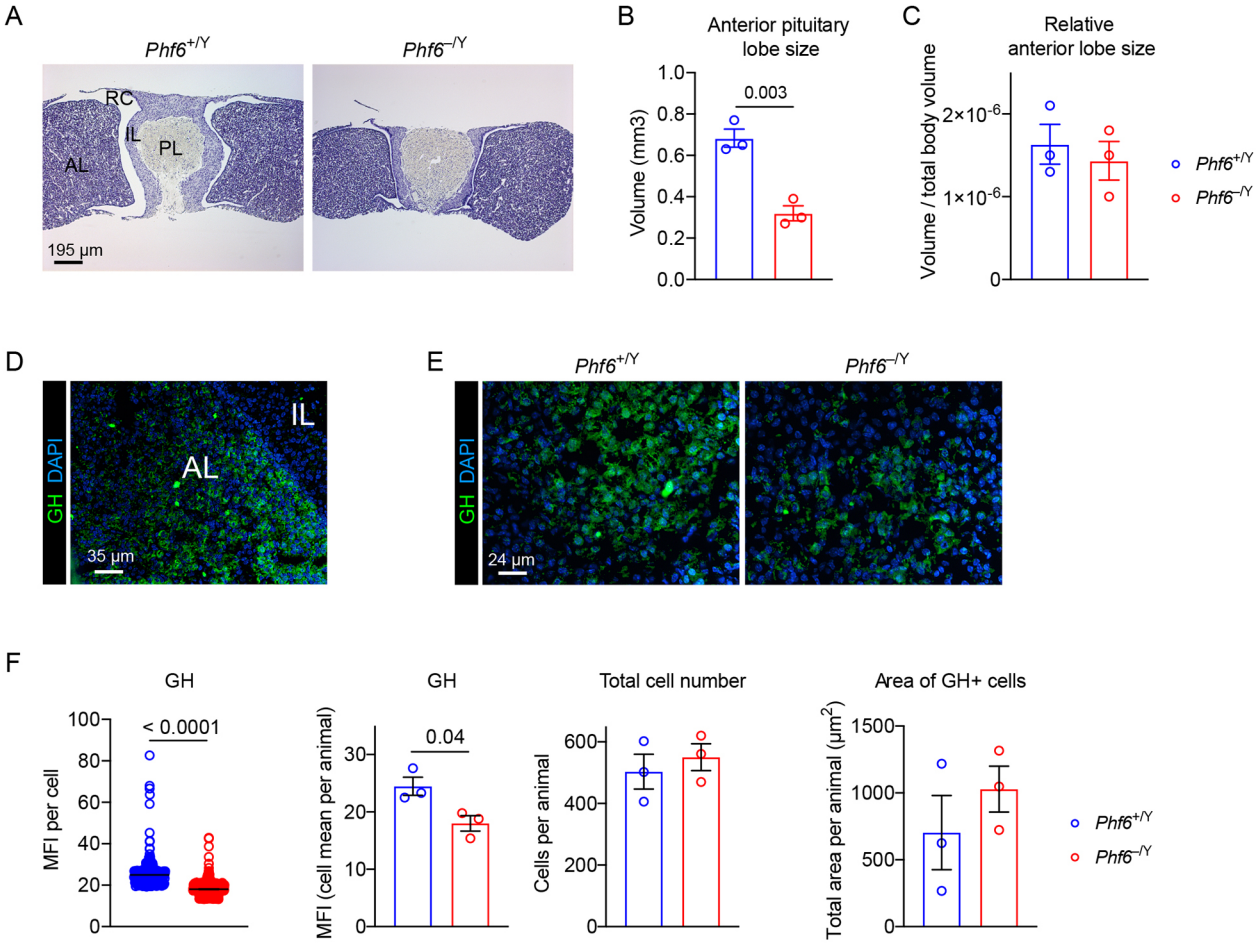

Fig. 5. GH levels per cell are reduced in the absence of PHF6. (A) Representative images of Cresyl Violet-stained horizontal sections of 4-week-old *Phf6*$^{+/Y}$ and *Phf6*$^{-/Y}$ pituitary glands. (B) Assessment of the volumes of the anterior lobes of *Phf6*$^{+/Y}$ and *Phf6*$^{-/Y}$ pituitary glands using the method described by Coggeshall (1992). (C) Volume of the anterior lobe of *Phf6*$^{+/Y}$ and *Phf6*$^{-/Y}$ pituitary glands relative to the total body volume. (D) Representative GH immunofluorescence image showing the specificity of the antibody detecting GH in the anterior lobe (AL), but not in the intermediate lobe (IL) of the pituitary gland, as expected. GH, green; DAPI, blue. (E) Representative higher magnification GH immunofluorescence images of the anterior lobe of the pituitary glands of 6- to 7-week-old *Phf6*$^{+/Y}$ and *Phf6*$^{-/Y}$ mice. (F) Numerical assessment of GH immunofluorescence intensity per cell and summarized per animal, as well as total cell number in the tissue area analyzed and area of GH^{+} cells in *Phf6*$^{+/Y}$ and *Phf6*$^{-/Y}$ pituitary glands. AL, anterior lobe; IL, intermediate lobe; PL, posterior lobe; RC Rathke's cleft. Data are mean±s.e.m. and were analyzed using an unpaired, two-tailed Student's *t*-test. *n*=3 animals per genotype (B,C,F). Each data point represents the result from one animal (B,C,F), except F (left panel), where it represents the result from one cell. For each of the three animals per genotype, 402 to 620 cells were assessed.

Development (2020) 147, dev187021. doi:10.1242/dev.187021

display gigantism and elevated *Igf1* levels in several tissues (Favre et al., 1999; Greenhalgh et al., 2005; Metcalf et al., 2000).

To investigate whether upregulation of the GHRH/GH/IGF1 pathway could rescue the growth defects of *Phf6*$^{-/Y}$ mice, we generated *Phf6*;*Socs2* double mutant mice and determined the effects of loss of SOCS2 on the *Phf6*$^{-/Y}$ growth defect. We bred the *Socs2*$^{-/-}$ mice for three generations onto the mixed FVB/BALB/c background. Strikingly, deletion of *Socs2* partially rescued the growth defect resulting from loss of PHF6, with a significant increase detected by multiple comparisons between *Phf6*$^{-/Y}$;*Socs2*$^{+/+}$ and *Phf6*$^{-/Y}$;*Socs2*$^{-/-}$ mice from 5 weeks of age onwards (11.71±1.65 g versus 16.98±1.30 g at 5 weeks, P=0.04; Fig. 6A, Table S8). After 8 weeks, there was no statistically significant difference between the double mutant *Phf6*$^{-/Y}$;*Socs2*$^{-/-}$ and wild-type *Phf6*$^{+/Y}$;*Socs2*$^{+/+}$ mice, demonstrating a distinct rescue (27.78±1.13 g versus 24.42±0.73 g, respectively at 8 weeks, P=0.29; Fig. 6A, Table S8). Consistent with an effect on skeletal growth, deletion of *Socs2* increased the femur length of *Phf6*$^{-/Y}$ mice (Fig. 6B,C). These results indicate that the growth defects caused by loss of PHF6 can be reversed by elevated GH signaling.

DISCUSSION

An analysis of 19 individuals with BFLS showed that 47% of BFLS males have a height that is more than two standard deviations below the population average (Turner et al., 2004). Body size is controlled by both environmental and genetic factors (Grasgruber et al., 2014; Grunauer and Jorge, 2018; Lango Allen et al., 2010; Perkins et al., 2016). Genetic variants that impact body size typically have either a described role in cell proliferation (Bicknell et al., 2011a,b; Griffith et al., 2008; Guernsey et al., 2011; Klingseisen and Jackson, 2011; Rauch et al., 2008) or endocrine function (Abuzzahab et al., 2003; Pfäffle and Klammt, 2011; Phillips et al., 2001; Pugliese-Pires et al., 2011; Wajnrajch et al., 1996; Wit et al., 2016). In this article, we have shown that PHF6 is an important regulator of postnatal growth, and that deletion of germline *Phf6* in mice models the short stature of individuals with BFLS. The proportional growth defect resulting from *Phf6* deletion specifically within the nervous system indicates that PHF6 controls growth at least in part through neuroendocrine regulation.

Role of PHF6 in regulating the GHRH/GH/IGF1 axis

We have demonstrated that the GHRH/GH/IGF1 axis is a key pathway downregulated by loss of PHF6. We identified reduced transcription of *Ghrh* in the brain, *Gh* in the pituitary gland and *Igf1* in the liver. As GHRH regulates the transcription and secretion of *Gh* (Barinaga et al., 1983), which in turn regulates transcription of *Igf1* (Lupu et al., 2001), it is possible that the effects on *Gh* and *Igf1* mRNA could be an indirect downstream result of the reduction in *Ghrh*. Indeed, if the primary effect was GH or IGF1 reduction, increased *Ghrh* expression would be expected, owing to alleviation of the negative-feedback loop (Phelps et al., 1993). Furthermore, the effect of *Phf6* deletion appears to be similar to the *Ghrh* (Alba and Salvatori, 2004), *Ghrhr* (Eicher and Beamer, 1976) and *Ghr* (Lupu et al., 2001; Meyer et al., 2004; Zhou et al., 1997) mutant mice, which display postnatal growth defects. In contrast, *Igf1* mutant mice are already ∼60% smaller than controls at birth (Baker et al., 1993; Liu et al., 1993; Powell-Braxton et al., 1993). These observations, combined with the finding that nervous system-specific deletion of *Phf6* is sufficient to cause a growth defect, are consistent with a primary effect of PHF6 on regulating *Ghrh*. Notwithstanding, it is possible that PHF6 may also play an additional role in regulating *Gh* expression in the pituitary gland

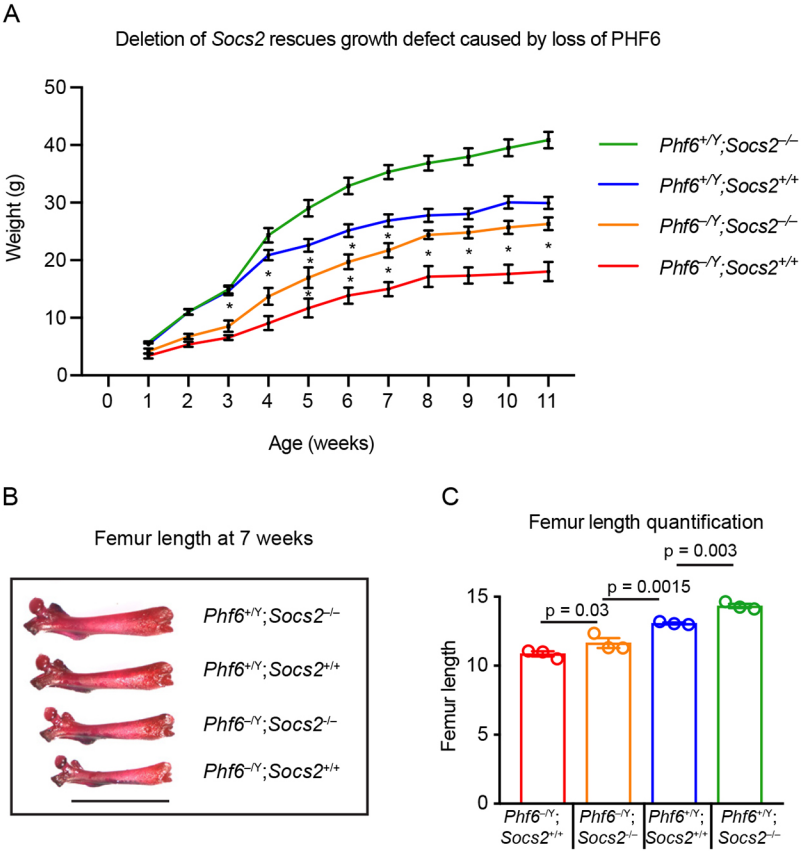

Fig. 6. Deletion of *Socs2* rescues the growth defect caused by loss of PHF6. (A) Weekly weight of mice of the indicated genotypes. Data are mean±s.e.m. and were analyzed using two-way ANOVA with age and genotype as the two independent factors and with Bonferroni's post-hoc test for multiple comparisons. *P<0.05 for multiple-comparisons between genotypes corresponding to lines on either side of the asterisk, only showing results for comparisons between *Phf6*$^{-/Y}$;*Socs2*$^{+/+}$ and *Phf6*$^{-/Y}$;*Socs2*$^{-/-}$ genotypes and comparisons between *Phf6*$^{-/Y}$;*Socs2*$^{-/-}$ and *Phf6*$^{+/Y}$;*Socs2*$^{+/+}$ genotypes. Full results from multiple comparison tests are presented in Table S8. n=4-9 animals per genotype. (B) Representative femurs stained with Alizarin Red S and Alcian Blue from mice of the indicated genotype. Scale bar: 10 mm. (C) Quantification of femur length in mice of the indicated genotype (units are mm). Results from each individual animal (n=3 per genotype) are indicated by a circle and data are mean±s.e.m. Data were analyzed using a one-way ANOVA with genotype as the independent factor and with Fisher's LSD test for multiple comparisons.

Development (2020) 147, dev187021. doi:10.1242/dev.187021

and *Igf1* in the liver, as *Phf6* is also expressed in these tissues (Voss et al., 2007). Further work is required to establish the exact molecular mechanisms by which PHF6 regulates endocrine pathways. Interestingly, PHF6 has been co-immunoprecipitated with PHIP (BRWD2), a reader of methylated H3K4 (Morgan et al., 2017), which has been shown to potentiate the effects of IGF1 signaling (Podcheko et al., 2007). *PHIP* mutations have been described in humans with developmental delay and intellectual disability (Jansen et al., 2018; Webster et al., 2016), while mice lacking the full-length PHIP protein display a postnatal growth defect (Li et al., 2010). Therefore, investigation into whether PHF6 interacts with PHIP to control the GH/IGF1 axis may offer insights towards our understanding of the molecular details of how PHF6 controls the GH/IGF1 pathway.

Rescue of the growth defect caused by loss of PHF6

The rescue of the growth defect in *Phf6*$^{-/Y}$ mice by additional deletion of *Socs2* demonstrates that loss of negative regulation of GH signaling is able to override the effects caused by loss of PHF6, supporting the hypothesis that PHF6 regulates the GHRH/GH/IGF1 axis. We conclude that the level of GH in the absence of PHF6 must be sufficient to enable the lack of negative regulation by SOCS2 to rescue the growth defect (in contrast to the *Ghrhr* knockout '*little*' mouse, in which the almost complete absence of GH renders mice unresponsive to deletion of *Socs2*) (Greenhalgh et al., 2005). These results provide a proof of principle that the growth defect caused by *Phf6* mutation can potentially be rescued with GH treatment. However, it will be important for clinicians to consider whether the potential benefits of GH treatment for humans with BFLS will outweigh the risks (Allen, 2006; Radcliffe et al., 2004). A 9-year-old female BFLS patient recently treated with daily growth hormone injections developed edema after 3 weeks of treatment (Zhang et al., 2019). Furthermore, treatment with growth enhancers must be carefully considered in the context of *PHF6* mutations being associated with leukemia (Van Vlierberghe et al., 2010). Two individuals with BFLS have developed hematopoietic malignancy (Carter et al., 2009; Chao et al., 2010). PHF6 regulates hematopoietic stem and progenitor cells (McRae et al., 2019; Wendorff et al., 2019), and notably, mice with germline or blood-specific mutation of *Phf6* have an accelerated onset of hematopoietic malignancy compared with controls (McRae et al., 2019), establishing PHF6 as a bona fide tumor suppressor. This indicates that other BFLS patients may be susceptible to leukemia. Although long-term studies have found no overall increased risk of leukemia with GH treatment in individuals with no known risk factors (Allen et al., 1997; Stochholm and Kiess, 2018), GH-treated patients with predisposing factors may be at higher risk (Nishi et al., 1999; Watanabe et al., 1993, 1988); thus, endocrine therapies for BFLS patients should be approached with consideration of these additional factors.

Role of PHF6 in regulating other hypothalamic-pituitary axis pathways

Despite having not observed a significant effect on PRL or ACTH secretion, we found that *Prl* and *Pomc* transcripts were downregulated in the pituitary gland and that PRL and ACTH levels per cell were reduced. Similarly, although we did not observe an effect on FSH or LH secretion, nor on mRNA levels, the levels of *Gnrh1* mRNA in the hypothalamus were reduced. The clinical signs of BFLS that these pathways may be related to (such as genital hypoplasia and gynecomastia) do not appear to manifest in mice. Any effect of PHF6 on these pathways at the transcriptional level appears to be compensated for, resulting in normal secretion levels in mice. Whether these pathways are important in the pathogenesis of human BFLS will be an important avenue for further research.

Mutation type and genetic background are important mediators of the effects of Phf6 mutation

At least three infants with BFLS have been treated for failure to thrive and a further two developed hypoglycaemia in the neonatal stage (Turner et al., 2004). Two deaths have been reported in childhood BFLS; one male at 2 years with severely retarded growth and another male at 4 years who presented with a respiratory illness (Birrell et al., 2003; Turner et al., 2004). No direct correlation between the specific *PHF6* mutation and the severity of presentation has been defined for BFLS in humans (Turner et al., 2004). The survival of PHF6^{C99F} hypomorphic mutant mice on the C57BL/6 background (Cheng et al., 2018), in contrast to the perinatal death of C57BL/6 mice with loss of function *Phf6* mutation reported here and in another loss of function *Phf6* model (Cheng et al., 2018), suggests that there is indeed an effect of mutation type on phenotypic presentation. The survival of FVB/BALB/c *Phf6*$^{-/Y}$ males shown here in contrast to the perinatal death of C57BL/6 *Phf6*$^{-/Y}$ males implicates the genetic background as an important additional mediator of the severity of phenotype presentation. Therefore, the specific *PHF6* mutation inherited in addition to the overall genetic makeup of the individual is likely to influence the presentation of clinical signs in BFLS. Environmental factors are also likely to mediate the impact of PHF6 mutations, as it has recently been shown that loss of PHF6 specifically in AgRP neurons has no effect on body weight in mice on an *ad libitum* diet; however, mice lacking PHF6 in AgRP neurons on an alternate fasting/feeding diet have reduced feeding and reduced body weight (Gan et al., 2020).

Overall, we have shown that PHF6 positively controls postnatal growth, at least in part through neuroendocrine signaling. We have demonstrated that PHF6 is an important regulator of the GHRH/GH/IGF1 axis; specifically, of levels of pituitary GH and secreted GH, and of *Ghrh*, *Gh* and *Igf1* transcripts. This study provides a better understanding of the etiology of BFLS and further insight into the genetic control of the endocrine system.

MATERIALS AND METHODS

Animals

The *Phf6*^{lox} targeted deletion allele has been previously described (McRae et al., 2019) and was used in combination with cre-deleter mice (Schwenk et al., 1995) for germline deletion. The *Nestin-cre* transgene (Tronche et al., 1999) was crossed to *Phf6* mice with the *Phf6*^{lox} targeted deletion allele mice maintained on a C57BL/6 background. As hemizygous *Phf6* deletion is perinatal lethal on a C57BL/6 background (McRae et al., 2019), mice were crossed to F1 hybrid FVB/BALB/c mice, as carried out previously (Thomas et al., 2006), and kept on a mixed genetic background with 50% FVB and 50% BALB/c contribution by crossing to F1 hybrid FVB/BALB/c mice in every generation. C57BL/6 mice with the *Socs2* null allele (Metcalf et al., 2000) were crossed for at least three generations to F1 FVB/BALB/c mice prior to experimental use. Genotyping was performed using primers as described in Table S9. All experimental procedures complied with the animal ethics regulations of the NHMRC of Australia and with approval of the WEHI Animal Ethics Committee.

Inclusion, exclusion and randomization

No animals were excluded. Where possible, automated assessment was used to avoid biases, e.g. multiplex hormone assays, automated image analysis (micro-CT, immunofluorescence), densitometry of western blots and RT-qPCR.

Repeat blood sampling

The sampling procedure, adapted from Steyn and colleagues (Steyn et al., 2011) used a modified version of the tail-clip blood collection procedure

Development (2020) 147, dev187021. doi:10.1242/dev.187021

(Abatan et al., 2008). A scalpel blade was used to create a small (1-2 mm) cut at the tail tip, followed by the collection of 4 µl of whole blood using a P20 pipette from the tail tip every 10 min over 6 h. Blood (4 µl) was added to 22 µl of 3.38 mM EDTA in PBS, immediately spun for 5 min at 2000 ***g*** to isolate the supernatant, which was snap frozen on dry ice before being stored at −80°C until analysis. The experiment was repeated a total of three times, with each experiment involving one *Phf6*$^{-/Y}$ animal and a *Phf6*$^{+/Y}$ littermate control.

Micro-CT assessment of body composition

Mice were imaged using a Bruker Skyscan 1276 Micro-CT system. Imaging parameters were set to balance contrast with acquisition time and resolution, and images were acquired with 41 µm^3 voxels. The x-ray projection images were reconstructed into 3D volumes using Bruker's NRecon software, before being analyzed in FIJI using a custom-written macro. Briefly, the images were run through a series of intensity and morphology filters, before being thresholded to remove signal from bone, skin and other organs. Total volumes of the animal, as well as the adipose tissue were recorded.

Hormone assay and data analysis

The multiplex pituitary hormone assay (MPTMAG-49K, Millipore) with beads to ACTH, FSH, GH, prolactin, TSH and LH was performed as per the manufacturer's instructions, in technical duplicates for each time point. The plates were read on the Luminex 200 3.1 xPONENT System. Standard curves and concentration values were obtained using the Milliplex Analyst 5.1 Software. Technical duplicates were averaged prior to deconvolution analysis and only excluded in the rare cases where no value for that analyte was returned from the multiplex assay. Precision values for the AutoDecon program were calculated as described (Johnson et al., 2008) using the minimal detectable concentration and the coefficient of variation values provided by the multiplex kit manufacturer. The AutoDecon algorithm (Johnson et al., 2008, 2009) was run independently for each animal and hormone with the peak triage *P*-value set to 0.15 and software-estimated values for the secretion standard deviation and the half-life. Serum IGF1 levels were measured using a Quantikine ELISA kit for IGF1 (R&D Systems, MG100) according to the manufacturer's instructions.

Western blot

Pituitary gland lysates were derived from micro dissected pituitary glands using KALB lysis buffer [1% Triton X, 1 mM EDTA, 150 mM NaCl, 50 mM Tris HCl (pH 7.4), 0.02% NaN_3] and proteinase inhibitors (Roche). Denatured lysates were separated by electrophoresis on a 4-12% NuPAGE Bis-Tris gel, and transferred onto a PVDF membrane (Osmonics). Membranes were blocked with 5% skim-milk/PBST, probed with anti-GH IgY antibody (XW-7687, Pro-Sci) followed by anti-IgY-HRP secondary (sc-2428, Santa Cruz) or anti-actin-HRP (sc-1616, Santa Cruz). Blots were developed on film using chemiluminescence and scanned for densitometry.

Immunofluorescence

Pituitary glands were dissected and positioned horizontally in cryomolds (Tissue-Tek, Y557) pre-filled with OCT mounting medium (Tissue-Tek, IA018) then immediately snap-frozen on dry ice before storage at −80°C. Specimens were sectioned in 5 µm sections using a Microm HM525 Cryostat and placed on Superfrost positively charged slides, air-dried briefly, then placed on dry ice and stored at −80°C.

For immunofluorescence staining, frozen sections were fixed in 4% (w/v) PFA (Sigma, 158127-500G) in phosphate-buffered saline (PBS) for 30 min, followed by permeabilization in 0.2% (v/v) Triton-X-100 (Sigma, T8787), then blocking in PBSG [0.25% (w/v) gelatine (Sigma, G-1890) in PBS] for 15 min each. Sections were incubated with primary antibody diluted in PBSG for 1 h in a wet chamber at room temperature. Antibodies used were raised against GH (XW-7687, Pro-Sci; 1:100), ACTH (orb10034, Biorbyt; 1:25), prolactin (orb4237, Biorbyt; 1:20), FSH (MA5-14711, Thermo Fisher; 1:50) and TSH (LS-C50523, Lifespan Biosciences; 1:100).

Thereafter, sections were washed three times in PBS for 5 min each, then incubated with secondary antibody for 1 h. Sections were rinsed in PBS and counterstained with 0.1 µg/ml of DAPI (Sigma, 10236276001) for 5 min at room temperature, rinsed in PBS then mounted with Dako fluorescence mounting medium (Dako, S3032). Slides were stored in the dark at 4°C and imaged 1-3 days after staining. Images were acquired on a compound fluorescence microscope (Axioplan 2, Zeiss) using a digital camera (AxioCam HR, Zeiss). Mean fluorescence intensity per cell was determined in areas of 112,230 µm^2 to 142,800 µm^2 per animal (corresponding to 3 to 4 40× view fields) using Image J (version 2.0.0-rc-39/1.50b). Grayscale images were thresholded, and hormone$^+$ and DAPI$^+$ particles of at least 3.2 µm^2 were measured.

RNA isolation and cDNA synthesis

Liver, brain, kidney and testis RNA were isolated by guanidine hydrochloride extraction and differential precipitation as described previously (Thomas and Dziadek, 1993). Pituitary gland RNA was isolated using an RNeasy mini kit (Qiagen) as per the manufacturer's instructions. RNA quality was assayed using the Agilent 2100 Bioanalyzer or the Agilent 4200 Tapestation, and samples with an RNA integrity number of less than 7 were not used for analysis. cDNA synthesis was performed using Superscript III (18080-085, Invitrogen) according to the manufacturer's instructions.

Northern blot

RNA (10 µg) was denatured in RNA loading buffer [200 µl 10× MOPS buffer (pH 7.0), 350 µl formaldehyde, 1000 µl formamide] at 55°C for 15 min. Samples were loaded with 2 µl of gel loading dye [50% (v/v) glycerol, 1 mM EDTA (pH 8.0), 0.25% bromophenol blue and 0.2% xyan cyanol in MQ-H_2O] and separated by gel electrophoresis (1% ultra-pure agarose, 18% formaldehyde, 10% MOPS buffer, recirculating) at 40 V overnight. Following separation, the gel was washed, then stained in 0.5 µg/ml ethidium bromide. The gel was de-stained in distilled H_2O then photographed using an ultraviolet trans-illuminator. RNA was transferred to a Hybond-N nylon membrane (Amersham Pharmacia Biotech) overnight, dried in an oven at 80°C for 1 h and cross-linked with 50 mJ of UV-light using the GS gene linker (BioRad, Hercules). A *Phf6* cDNA template corresponding to a region within exon 11, bases 2377 to 3156 of the published *Phf6* sequence (GenBank Accession Number NM_027642) was incubated with *in vitro* DNA polymerase reagents (Megaprime DNA Labelling System, Amersham Biosciences) and ^{32}P-dCTP (EasyTides, PerkinElmer). Synthesized radiolabeled probes were added to 10 ml of preheated hybridization buffer and incubated with the nylon membrane at 65°C overnight. After washing steps the membrane was exposed to X-ray film for 7 days at −70°C.

qPCR

Genomic DNA or cDNA was added to 10 µl, SensiMix SYBR (Bioline Reagents), 10 pmol each of a forward and reverse primer (Tables S10 and S11) designed using Primer3 (Koressaar and Remm, 2007; Untergasser et al., 2012), and 6 µl MilliQ-H_2O in a LightCycler 480 384-well Plate (Roche). Data were acquired on the LightCycler 480 (Roche) under the following conditions: one cycle of 95°C for 10 min; and 40 cycles of 95°C for 20 s, 60°C for 20 s, 72°C for 30 s. Standard curves based on arbitrary units corresponding to the Cp values obtained from serially diluted standard samples were used to calculate the initial concentration of the unknown samples. All samples were assayed in technical triplicates that were averaged prior to normalization with housekeeping gene(s): *B2m* for genomic DNA, and *Gapdh* and/or *Pgk1* for RT-qPCR. A triplicate measurement was excluded in the rare case where there was a greater than 20% difference compared with the other two replicates for a particular sample (and the average of the other two replicates only was used for analysis).

Skeletal preparations

Skeletal preparations were performed as previously described (Voss et al., 2009), using a protocol adapted from Kaufman (1992). Specifically, adult carcasses were skinned, fixed in ethanol for 7 days, followed by acetone for 7 days. Subsequently, specimens were stained for 10 days in a solution containing 1 volume of 0.4% Alcian Blue in 70% ethanol, 1 volume of glacial acetic acid, 14 volumes of 95% ethanol, 4 volumes of H_2O and 0.2 volumes of 0.5% Alizarin Red S in H_2O. Samples were rinsed, then kept in a

solution of 20% glycerol and 1% potassium hydroxide for 3 days at 37°C, then for 4 days at room temperature. Skeletons were transferred to 50% glycerol prior to imaging and femur length quantification.

Statistical analysis

Statistical analysis, including unpaired (paired in Table 1) *t*-tests, Chi-squared tests and ANOVA, were performed using Prism 8.

Acknowledgements

We thank F. Dabrowski, G. Panoschi, L. Johnson, L. Wilkins and WEHI Bioservices for assistance with animal experiments; M. Corbett and M. Dixon for creating the *Phf6* targeted construct; and J. Chue for preliminary work on the *Phf6* mutant mice. We thank R. E. May, H. Pehlivanoglu and L. Potenza for excellent technical support. We are grateful to E. Bandala-Sanchez and T. A. Nguyen for assistance with the multiplex assay, and to G. Schütz for providing the Nestin-cre transgenic mice.

Competing interests

The authors declare no competing or financial interests.

Author contributions

Conceptualization: T.T., A.K.V.; Methodology: S.E., L.W.; Formal analysis: H.M.M., L.W., A.K.V.; Investigation: H.M.M., S.E., L.W.; Resources: W.S.A., J.G.; Data curation: H.M.M.; Writing - original draft: H.M.M.; Writing - review & editing: W.S.A., J.G., T.T., A.K.V.; Visualization: H.M.M.; Supervision: T.T., A.K.V.; Project administration: H.M.M.; Funding acquisition: T.T., A.K.V.

Funding

This work was supported by an Australian Postgraduate Award (H.M.M.), by National Health and Medical Research Council (NHMRC) project grants (1029481 to A.K.V. and T.T., and 1161111 to A.K.V.), by National Health and Medical Research Council program grants (1091593 to J.G. and 1113577 to W.S.A.), by a National Health and Medical Research Council investigator grant (1176789 to A.K.V.), by a National Health and Medical Research Council research fellowships (1003435 to T.T., 575512 and 1081421 to A.K.V., 1155224 to J.G., and 1058344 to W.S.A.), by the Independent Research Institutes Infrastructure Support Scheme from the Australian Government's National Health and Medical Research Council, and by a Victorian State Government Operational Infrastructure Support Grant.

Supplementary information

Supplementary information available online at
https://dev.biologists.org/lookup/doi/10.1242/dev.187021.supplemental

Peer review history

The peer review history is available online at
https://dev.biologists.org/lookup/doi/10.1242/dev.187021.reviewer-comments.pdf

References

Aasland, R., Gibson, T. J. and Stewart, A. F. (1995). The PHD finger: implications for chromatin-mediated transcriptional regulation. *Trends Biochem. Sci.* **20**, 56-59. doi:10.1016/S0968-0004(00)88957-4

Abatan, O. I., Welch, K. B. and Nemzek, J. A. (2008). Evaluation of saphenous venipuncture and modified tail-clip blood collection in mice. *J. Am. Assoc. Lab. Anim. Sci.* **47**, 8-15.

Abuzzahab, M. J., Schneider, A., Goddard, A., Grigorescu, F., Lautier, C., Keller, E., Kiess, W., Klammt, J., Kratzsch, J., Osgood, D. et al. (2003). IGF-I receptor mutations resulting in intrauterine and postnatal growth retardation. *N. Engl. J. Med.* **349**, 2211-2222. doi:10.1056/NEJMoa010107

Alba, M. and Salvatori, R. (2004). A mouse with targeted ablation of the growth hormone-releasing hormone gene: a new model of isolated growth hormone deficiency. *Endocrinology* **145**, 4134-4143. doi:10.1210/en.2004-0119

Allen, D. B. (2006). Growth hormone therapy for short stature: is the benefit worth the burden? *Pediatrics* **118**, 343-348. doi:10.1542/peds.2006-0329

Allen, D. B., Rundle, A. C., Graves, D. A. and Blethen, S. L. (1997). Risk of leukemia in children treated with human growth hormone: review and reanalysis. *J. Pediatr.* **131**, S32-S36. doi:10.1016/S0022-3476(97)70008-8

Ardinger, H. H., Hanson, J. W. and Zellweger, H. U. (1984). Börjeson-Forssman-Lehmann syndrome: further delineation in five cases. *Am. J. Med. Genet.* **19**, 653-664. doi:10.1002/ajmg.1320190405

Baker, J., Liu, J.-P., Robertson, E. J. and Efstratiadis, A. (1993). Role of insulin-like growth factors in embryonic and postnatal growth. *Cell* **75**, 73-82. doi:10.1016/S0092-8674(05)80085-6

Barinaga, M., Yamonoto, G., Rivier, C., Vale, W., Evans, R. and Rosenfeld, M. G. (1983). Transcriptional regulation of growth hormone gene expression by growth hormone-releasing factor. *Nature* **306**, 84-85. doi:10.1038/306084a0

Baumstark, A., Lower, K. M., Sinkus, A., Andriuskeviciute, I., Jurkeniene, L., Gecz, J. and Just, W. (2003). Novel PHF6 mutation p.D333del causes Borjeson-Forssman-Lehmann syndrome. *J. Med. Genet.* **40**, e50. doi:10.1136/jmg.40.4.e50

Berland, S., Alme, K., Brendehaug, A., Houge, G. and Hovland, R. (2011). PHF6 deletions may cause Borjeson-Forssman-Lehmann syndrome in females. *Mol. Syndromol.* **1**, 294-300. doi:10.1159/000330111

Bernard, V., Young, J. and Binart, N. (2019). Prolactin - a pleiotropic factor in health and disease. *Nat. Rev. Endocrinol.* **15**, 356-365. doi:10.1038/s41574-019-0194-6

Bicknell, L. S., Bongers, E. M. H. F., Leitch, A., Brown, S., Schoots, J., Harley, M. E., Aftimos, S., Al-Aama, J. Y., Bober, M., Brown, P. A. J. et al. (2011a). Mutations in the pre-replication complex cause Meier-Gorlin syndrome. *Nat. Genet.* **43**, 356-359. doi:10.1038/ng.775

Bicknell, L. S., Walker, S., Klingseisen, A., Stiff, T., Leitch, A., Kerzendorfer, C., Martin, C.-A., Yeyati, P., Al Sanna, N., Bober, M. et al. (2011b). Mutations in ORC1, encoding the largest subunit of the origin recognition complex, cause microcephalic primordial dwarfism resembling Meier-Gorlin syndrome. *Nat. Genet.* **43**, 350-355. doi:10.1038/ng.776

Birrell, G., Lampe, A., Richmond, S., Bruce, S. N., Gecz, J., Lower, K., Wright, M. and Cheetham, T. D. (2003). Borjeson-Forssman-Lehmann syndrome and multiple pituitary hormone deficiency. *J. Pediatr. Endocrinol. Metab.* **16**, 1295-1300. doi:10.1515/JPEM.2003.16.9.1295

Börjeson, M., Forssman, H. and Lehmann, O. (1962). An X-linked, recessively inherited syndrome characterized by grave mental deficiency, epilepsy, and endocrine disorder. *Acta Med. Scand.* **171**, 13-21. doi:10.1111/j.0954-6820.1962.tb04162.x

Carter, M. T., Picketts, D. J., Hunter, A. G. and Graham, G. E. (2009). Further clinical delineation of the Börjeson-Forssman-Lehmann syndrome in patients with PHF6 mutations. *Am. J. Med. Genet.* **149A**, 246-250. doi:10.1002/ajmg.a.32624

Chao, M. M., Todd, M. A., Kontny, U., Neas, K., Sullivan, M. J., Hunter, A. G., Picketts, D. J. and Kratz, C. P. (2010). T-cell acute Lymphoblastic Leukemia in Association With Börjeson-Forssman-Lehmann syndrome due to a mutation in PHF6. *Pediatr. Blood Cancer* **55**, 722-724. doi:10.1002/pbc.22574

Cheng, C., Deng, P.-Y., Ikeuchi, Y., Yuede, C., Li, D., Rensing, N., Huang, J., Baldridge, D., Maloney, S. E., Dougherty, J. D. et al. (2018). Characterization of a mouse model of Börjeson-Forssman-Lehmann syndrome. *Cell Rep* **25**, 1404-1414.e1406. doi:10.1016/j.celrep.2018.10.043

Chrousos, G. P., Kino, T. and Charmandari, E. (2009). Evaluation of the hypothalamic-pituitary-adrenal axis function in childhood and adolescence. *Neuroimmunomodulation* **16**, 272-283. doi:10.1159/000216185

Coggeshall, R. E. (1992). A consideration of neural counting methods. *Trends Neurosci.* **15**, 9-13. doi:10.1016/0166-2236(92)90339-A

Crawford, J., Lower, K. M., Hennekam, R. C. M., Van Esch, H., Megarbane, A., Lynch, S. A., Turner, G. and Gecz, J. (2006). Mutation screening in Borjeson-Forssman-Lehmann syndrome: identification of a novel de novo PHF6 mutation in a female patient. *J. Med. Genet.* **43**, 238-243. doi:10.1136/jmg.2005.033084

de Winter, C. F., van Dijk, F., Stolker, J. J. and Hennekam, R. C. M. (2009). Behavioural phenotype in Börjeson-Forssman-Lehmann syndrome. *J. Intellect. Disabil. Res.* **53**, 319-328. doi:10.1111/j.1365-2788.2009.01156.x

Declercq, J., Brouwers, B., Pruniau, V. P. E. G., Stijnen, P., de Faudeur, G., Tuand, K., Meulemans, S., Serneels, L., Schraenen, A., Schuit, F. et al. (2015). Metabolic and behavioural phenotypes in Nestin-Cre mice are caused by hypothalamic expression of human growth hormone. *PLoS ONE* **10**, e0135502. doi:10.1371/journal.pone.0135502

Dereymaeker, A. M., Fryns, J. P., Hoefnagels, M., Heremans, G., Marien, J. and van den Berghe, H. (1986). The Borjeson-Forssman-Lehmann syndrome. A family study. *Clin. Genet.* **29**, 317-320. doi:10.1111/j.1399-0004.1986.tb01260.x

Eicher, E. M. and Beamer, W. G. (1976). Inherited ateliotic dwarfism in mice: characteristics of the mutation, little, on chromosome 6. *J. Hered.* **67**, 87-91. doi:10.1093/oxfordjournals.jhered.a108682

Favre, H., Benhamou, A., Finidori, J., Kelly, P. A. and Edery, M. (1999). Dual effects of suppressor of cytokine signaling (SOCS-2) on growth hormone signal transduction. *FEBS Lett.* **453**, 63-66. doi:10.1016/S0014-5793(99)00681-X

Galichet, C., Lovell-Badge, R. and Rizzoti, K. (2010). Nestin-Cre mice are affected by hypopituitarism, which is not due to significant activity of the transgene in the pituitary gland. *PLoS ONE* **5**, e11443. doi:10.1371/journal.pone.0011443

Gan, L., Sun, J., Yang, S., Zhang, X., Chen, W., Sun, Y., Wu, X., Cheng, C., Yuan, J., Li, A. et al. (2020). Chromatin-binding protein PHF6 regulates activity-dependent transcriptional networks to promote hunger response. *Cell Rep.* **30**, 3717-3728.e3716. doi:10.1016/j.celrep.2020.02.085

Gécz, J., Turner, G., Nelson, J. and Partington, M. (2006). The Börjeson-Forssman-Lehman syndrome (BFLS, MIM #301900). *Eur. J. Hum. Genet.* **14**, 1233-1237. doi:10.1038/sj.ejhg.5201639

Grasgruber, P., Cacek, J., Kalina, T. and Sebera, M. (2014). The role of nutrition and genetics as key determinants of the positive height trend. *Econ. Hum. Biol.* **15**, 81-100. doi:10.1016/j.ehb.2014.07.002

Greenhalgh, C. J., Rico-Bautista, E., Lorentzon, M., Thaus, A. L., Morgan, P. O., Willson, T. A., Zervoudakis, P., Metcalf, D., Street, I., Nicola, N. A. et al. (2005).

SOCS2 negatively regulates growth hormone action in vitro and in vivo. *J. Clin. Invest.* **115**, 397-406. doi:10.1172/JCI200522710

Griffith, E., Walker, S., Martin, C.-A., Vagnarelli, P., Stiff, T., Vernay, B., Al Sanna, N., Saggar, A., Hamel, B., Earnshaw, W. C. et al. (2008). Mutations in pericentrin cause Seckel syndrome with defective ATR-dependent DNA damage signaling. *Nat. Genet.* **40**, 232-236. doi:10.1038/ng.2007.80

Grunauer, M. and Jorge, A. A. L. (2018). Genetic short stature. *Growth Horm. IGF Res.* **38**, 29-33. doi:10.1016/j.ghir.2017.12.003

Guernsey, D. L., Matsuoka, M., Jiang, H., Evans, S., Macgillivray, C., Nightingale, M., Perry, S., Ferguson, M., LeBlanc, M., Paquette, J. et al. (2011). Mutations in origin recognition complex gene ORC4 cause Meier-Gorlin syndrome. *Nat. Genet.* **43**, 360-364. doi:10.1038/ng.777

Hsu, Y.-C., Chen, T.-C., Lin, C.-C., Yuan, C.-T., Hsu, C.-L., Hou, H.-A., Kao, C.-J., Chuang, P.-H., Chen, Y.-R., Chou, W.-C. et al. (2019). Phf6-null hematopoietic stem cells have enhanced self-renewal capacity and oncogenic potentials. *Blood Adv.* **3**, 2355-2367. doi:10.1182/bloodadvances.2019000391

Ikegami, K. and Yoshimura, T. (2017). The hypothalamic-pituitary-thyroid axis and biological rhythms: The discovery of TSH's unexpected role using animal models. *Best Pract. Res. Clin. Endocrinol. Metab.* **31**, 475-485. doi:10.1016/j.beem.2017.09.002

Jansen, S., Hoischen, A., Coe, B. P., Carvill, G. L., Van Esch, H., Bosch, D. G. M., Andersen, U. A., Baker, C., Bauters, M., Bernier, R. A. et al. (2018). A genotype-first approach identifies an intellectual disability-overweight syndrome caused by PHIP haploinsufficiency. *Eur. J. Hum. Genet.* **26**, 54-63. doi:10.1038/s41431-017-0039-5

Johnson, M. L., Pipes, L., Veldhuis, P. P., Farhy, L. S., Boyd, D. G. and Evans, W. S. (2008). AutoDecon, a deconvolution algorithm for identification and characterization of luteinizing hormone secretory bursts: description and validation using synthetic data. *Anal. Biochem.* **381**, 8-17. doi:10.1016/j.ab.2008.07.001

Johnson, M. L., Pipes, L., Veldhuis, P. P., Farhy, L. S., Nass, R., Thorner, M. O. and Evans, W. S. (2009). AutoDecon: a robust numerical method for the quantification of pulsatile events. *Methods Enzymol.* **454**, 367-404. doi:10.1016/S0076-6879(08)03815-9

Kaufman, M. H. (1992). *The Atlas of Mouse Development*: Elsevier.

Klingseisen, A. and Jackson, A. P. (2011). Mechanisms and pathways of growth failure in primordial dwarfism. *Genes Dev.* **25**, 2011-2024. doi:10.1101/gad.169037

Koressaar, T. and Remm, M. (2007). Enhancements and modifications of primer design program Primer3. *Bioinformatics* **23**, 1289-1291. doi:10.1093/bioinformatics/btm091

Lango Allen, H., Estrada, K., Lettre, G., Berndt, S. I., Weedon, M. N., Rivadeneira, F., Willer, C. J., Jackson, A. U., Vedantam, S., Raychaudhuri, S. et al. (2010). Hundreds of variants clustered in genomic loci and biological pathways affect human height. *Nature* **467**, 832-838. doi:10.1038/nature09410

Li, S., Francisco, A. B., Han, C., Pattabiraman, S., Foote, M. R., Giesy, S. L., Wang, C., Schimenti, J. C., Boisclair, Y. R. and Long, Q. (2010). The full-length isoform of the mouse pleckstrin homology domain-interacting protein (PHIP) is required for postnatal growth. *FEBS Lett.* **584**, 4121-4127. doi:10.1016/j.febslet.2010.08.042

Linossi, E. M., Babon, J. J., Hilton, D. J. and Nicholson, S. E. (2013). Suppression of cytokine signaling: the SOCS perspective. *Cytokine Growth Factor. Rev.* **24**, 241-248. doi:10.1016/j.cytogfr.2013.03.005

Liu, J.-P., Baker, J., Perkins, A. S., Robertson, E. J. and Efstratiadis, A. (1993). Mice carrying null mutations of the genes encoding insulin-like growth factor I (Igf-1) and type 1 IGF receptor (Igf1r). *Cell* **75**, 59-72. doi:10.1016/S0092-8674(05)80084-4

Lower, K. M., Turner, G., Kerr, B. A., Mathews, K. D., Shaw, M. A., Gedeon, A. K., Schelley, S., Hoyme, H. E., White, S. M., Delatycki, M. B. et al. (2002). Mutations in PHF6 are associated with Börjeson-Forssman-Lehmann syndrome. *Nat. Genet.* **32**, 661-665. doi:10.1038/ng1040

Lupu, F., Terwilliger, J. D., Lee, K., Segre, G. V. and Efstratiadis, A. (2001). Roles of growth hormone and insulin-like growth factor 1 in mouse postnatal growth. *Dev. Biol.* **229**, 141-162. doi:10.1006/dbio.2000.9975

Matsuo, K., Murano, I. and Kajii, T. (1984). Borjeson-Forssman-Lehmann syndrome in a girl. *Jap. J. Hum. Genet.* **29**, 121-126. doi:10.1007/BF01873532

McRae, H. M., Garnham, A. L., Hu, Y., Witkowski, M. T., Corbett, M. A., Dixon, M. P., May, R. E., Sheikh, B. N., Chiang, W., Kueh, A. J. et al. (2019). PHF6 regulates hematopoietic stem and progenitor cells and its loss synergizes with expression of TLX3 to cause leukemia. *Blood* **133**, 1729-1741. doi:10.1182/blood-2018-07-860726

Metcalf, D., Greenhalgh, C. J., Viney, E., Willson, T. A., Starr, R., Nicola, N. A., Hilton, D. J. and Alexander, W. S. (2000). Gigantism in mice lacking suppressor of cytokine signalling-2. *Nature* **405**, 1069-1073. doi:10.1038/35016611

Meyer, C. W. E., Korthaus, D., Jagla, W., Cornali, E., Grosse, J., Fuchs, H., Klingenspor, M., Roemheld, S., Tschöp, M., Heldmaier, G. et al. (2004). A novel missense mutation in the mouse growth hormone gene causes semidominant dwarfism, hyperghrelinemia, and obesity. *Endocrinology* **145**, 2531-2541. doi:10.1210/en.2003-1125

Miyagi, S., Sroczynska, P., Kato, Y., Nakajima-Takagi, Y., Oshima, M., Rizq, O., Takayama, N., Saraya, A., Mizuno, S., Sugiyama, F. et al. (2019). The chromatin-binding protein Phf6 restricts the self-renewal of hematopoietic stem cells. *Blood* **133**, 2495-2506. doi:10.1182/blood.2019000468

Morgan, M. A. J., Rickels, R. A., Collings, C. K., He, X., Cao, K., Herz, H.-M., Cozzolino, K. A., Abshiru, N. A., Marshall, S. A., Rendleman, E. J. et al. (2017). A cryptic Tudor domain links BRWD2/PHIP to COMPASS-mediated histone H3K4 methylation. *Genes Dev.* **31**, 2003-2014. doi:10.1101/gad.305201.117

Nishi, Y., Tanaka, T., Takano, K., Fujieda, K., Igarashi, Y., Hanew, K., Hirano, T., Yokoya, S., Tachibana, K., Saito, T. et al. (1999). Recent status in the occurrence of leukemia in growth hormone-treated patients in Japan. *J. Clin. Endocrinol. Metab.* **84**, 1961-1965. doi:10.1210/jcem.84.6.5716

Oh, S., Boo, K., Kim, J., Baek, S. A., Jeon, Y., You, J., Lee, H., Choi, H.-J., Park, D., Lee, J. M. et al. (2020). The chromatin-binding protein PHF6 functions as an E3 ubiquitin ligase of H2BK120 via H2BK12Ac recognition for activation of trophectodermal genes. *Nucleic Acids Res.* **48**, 9037-9052. doi:10.1093/nar/gkaa626

Perkins, J. M., Subramanian, S. V., Davey Smith, G. and Özaltin, E. (2016). Adult height, nutrition, and population health. *Nutr. Rev.* **74**, 149-165. doi:10.1093/nutrit/nuv105

Petridou, M., Kimiskidis, V., Deligiannis, K. and Kazis, A. (1997). Borjeson-Forssman-Lehmann syndrome: two severely handicapped females in a family. *Clin. Neurol. Neurosurg.* **99**, 148-150. doi:10.1016/S0303-8467(97)80014-5

Pfäffle, R. and Klammt, J. (2011). Pituitary transcription factors in the aetiology of combined pituitary hormone deficiency. *Best Pract. Res. Clin. Endocrinol. Metab.* **25**, 43-60. doi:10.1016/j.beem.2010.10.014

Phelps, C. J., Dalcik, H., Endo, H., Talamantes, F. and Hurley, D. L. (1993). Growth hormone-releasing hormone peptide and mRNA are overexpressed in GH-deficient Ames dwarf mice. *Endocrinology* **133**, 3034-3037. doi:10.1210/endo.133.6.7694848

Phillips, S. A., Rotman-Pikielny, P., Lazar, J., Ando, S., Hauser, P., Skarulis, M. C., Brucker-Davis, F. and Yen, P. M. (2001). Extreme thyroid hormone resistance in a patient with a novel truncated TR mutant. *J. Clin. Endocrinol. Metab.* **86**, 5142-5147. doi:10.1210/jcem.86.11.8051

Podcheko, A., Northcott, P., Bikopoulos, G., Lee, A., Bommareddi, S. R., Kushner, J. A., Farhang-Fallah, J. and Rozakis-Adcock, M. (2007). Identification of a WD40 repeat-containing isoform of PHIP as a novel regulator of β-cell growth and survival. *Mol. Cell. Biol.* **27**, 6484-6496. doi:10.1128/MCB.02409-06

Powell-Braxton, L., Hollingshead, P., Warburton, C., Dowd, M., Pitts-Meek, S., Dalton, D., Gillett, N. and Stewart, T. A. (1993). IGF-I is required for normal embryonic growth in mice. *Genes Dev.* **7**, 2609-2617. doi:10.1101/gad.7.12b.2609

Pugliese-Pires, P. N., Fortin, J.-P., Arthur, T., Latronico, A. C., Mendonca, B. B., Villares, S. M. F., Arnhold, I. J. P., Kopin, A. S. and Jorge, A. A. L. (2011). Novel inactivating mutations in the GH secretagogue receptor gene in patients with constitutional delay of growth and puberty. *Eur. J. Endocrinol.* **165**, 233-241. doi:10.1530/EJE-11-0168

Radcliffe, D. J., Pliskin, J. S., Silvers, J. B. and Cuttler, L. (2004). Growth hormone therapy and quality of life in adults and children. *Pharmacoeconomics* **22**, 499-524. doi:10.2165/00019053-200422080-00003

Ranke, M. B. and Wit, J. M. (2018). Growth hormone - past, present and future. *Nat. Rev. Endocrinol.* **14**, 285-300. doi:10.1038/nrendo.2018.22

Rauch, A., Thiel, C. T., Schindler, D., Wick, U., Crow, Y. J., Ekici, A. B., van Essen, A. J., Goecke, T. O., Al-Gazali, L., Chrzanowska, K. H. et al. (2008). Mutations in the pericentrin (PCNT) gene cause primordial dwarfism. *Science* **319**, 816-819. doi:10.1126/science.1151174

Rico-Bautista, E., Flores-Morales, A. and Fernandez-Perez, L. (2006). Suppressor of cytokine signaling (SOCS) 2, a protein with multiple functions. *Cytokine Growth Factor. Rev.* **17**, 431-439. doi:10.1016/j.cytogfr.2006.09.008

Robinson, L. K., Jones, K. L., Culler, F., Nyhan, W. L., Sakati, N. and Jones, K. L. (1983). The Börjeson-Forssman-Lehmann syndrome. *Am. J. Med. Genet.* **15**, 457-468. doi:10.1002/ajmg.1320150311

Schwenk, F., Baron, U. and Rajewsky, K. (1995). A cre-transgenic mouse strain for the ubiquitous deletion of loxP-flanked gene segments including deletion in germ cells. *Nucleic Acids Res.* **23**, 5080-5081. doi:10.1093/nar/23.24.5080

Soto-Feliciano, Y. M., Bartlebaugh, J. M. E., Liu, Y. P., Sánchez-Rivera, F. J., Bhutkar, A., Weintraub, A. S., Buenrostro, J. D., Cheng, C. S., Regev, A., Jacks, T. E. et al. (2017). PHF6 regulates phenotypic plasticity through chromatin organization within lineage-specific genes. *Genes Dev.* **31**, 973-989. doi:10.1101/gad.295857.117

Stamatiades, G. A. and Kaiser, U. B. (2018). Gonadotropin regulation by pulsatile GnRH: Signaling and gene expression. *Mol. Cell. Endocrinol.* **463**, 131-141. doi:10.1016/j.mce.2017.10.015

Steyn, F. J., Huang, L., Ngo, S. T., Leong, J. W., Tan, H. Y., Xie, T. Y., Parlow, A. F., Veldhuis, J. D., Waters, M. J. and Chen, C. (2011). Development of a method for the determination of pulsatile growth hormone secretion in mice. *Endocrinology* **152**, 3165-3171. doi:10.1210/en.2011-0253

Steyn, F. J., Wan, Y., Clarkson, J., Veldhuis, J. D., Herbison, A. E. and Chen, C. (2013). Development of a methodology for and assessment of pulsatile luteinizing

hormone secretion in juvenile and adult male mice. *Endocrinology* **154**, 4939-4945. doi:10.1210/en.2013-1502

Stochholm, K. and Kiess, W. (2018). Long-term safety of growth hormone-A combined registry analysis. *Clin. Endocrinol.* **88**, 515-528. doi:10.1111/cen.13502

Thackray, V. G., Mellon, P. L. and Coss, D. (2010). Hormones in synergy: regulation of the pituitary gonadotropin genes. *Mol. Cell. Endocrinol.* **314**, 192-203. doi:10.1016/j.mce.2009.09.003

Thomas, T. and Dziadek, M. (1993). Capacity to form choroid plexus-like cells in vitro is restricted to specific regions of the mouse neural ectoderm. *Development* **117**, 253-262.

Thomas, T., Corcoran, L. M., Gugasyan, R., Dixon, M. P., Brodnicki, T., Nutt, S. L., Metcalf, D. and Voss, A. K. (2006). Monocytic leukemia zinc finger protein is essential for the development of long-term reconstituting hematopoietic stem cells. *Genes Dev.* **20**, 1175-1186. doi:10.1101/gad.1382606

Todd, M. A. M. and Picketts, D. J. (2012). PHF6 Interacts with the Nucleosome Remodeling and Deacetylation (NuRD) Complex. *J. Proteome Res.* **11**, 4326-4337. doi:10.1021/pr3004369

Tronche, F., Kellendonk, C., Kretz, O., Gass, P., Anlag, K., Orban, P. C., Bock, R., Klein, R. and Schütz, G. (1999). Disruption of the glucocorticoid receptor gene in the nervous system results in reduced anxiety. *Nat. Genet.* **23**, 99-103. doi:10.1038/12703

Turner, G., Gedeon, A., Mulley, J., Sutherland, G., Rae, J., Power, K. and Arthur, I. (1989). Börjeson-Forssman-Lehmann syndrome: clinical manifestations and gene localization to Xq26-27. *Am. J. Med. Genet.* **34**, 463-469. doi:10.1002/ajmg.1320340402

Turner, G., Lower, K. M., White, S. M., Delatycki, M., Lampe, A. K., Wright, M., Clayton-Smith, J., Kerr, B., Schelley, S., Hoyme, H. E. et al. (2004). The clinical picture of the Börjeson-Forssman-Lehmann syndrome in males and heterozygous females with PHF6 mutations. *Clin. Genet.* **65**, 226-232. doi:10.1111/j.0009-9163.2004.00215.x

Untergasser, A., Cutcutache, I., Koressaar, T., Ye, J., Faircloth, B. C., Remm, M. and Rozen, S. G. (2012). Primer3–new capabilities and interfaces. *Nucleic Acids Res.* **40**, e115. doi:10.1093/nar/gks596

Van Vlierberghe, P., Palomero, T., Khiabanian, H., Van der Meulen, J., Castillo, M., Van Roy, N., De Moerloose, B., Philippé, J., Gonzalez-García, S., Toribio, M. L. et al. (2010). PHF6 mutations in T-cell acute lymphoblastic leukemia. *Nat. Genet.* **42**, 338-342. doi:10.1038/ng.542

Van Vlierberghe, P., Patel, J., Abdel-Wahab, O., Lobry, C., Hedvat, C. V., Balbin, M., Nicolas, C., Payer, A. R., Fernandez, H. F., Tallman, M. S. et al. (2011). PHF6 mutations in adult acute myeloid leukemia. *Leukemia* **25**, 130-134. doi:10.1038/leu.2010.247

Voss, A. K., Gamble, R., Collin, C., Shoubridge, C., Corbett, M., Gécz, J. and Thomas, T. (2007). Protein and gene expression analysis of Phf6, the gene mutated in the Börjeson-Forssman-Lehmann Syndrome of intellectual disability and obesity. *Gene Expr. Patterns* **7**, 858-871. doi:10.1016/j.modgep.2007.06.007

Voss, A. K., Collin, C., Dixon, M. P. and Thomas, T. (2009). Moz and retinoic acid coordinately regulate H3K9 acetylation, Hox gene expression, and segment identity. *Dev. Cell* **17**, 674-686. doi:10.1016/j.devcel.2009.10.006

Wajnrajch, M. P., Gertner, J. M., Harbison, M. D., Chua, S. C., Jr and Leibel, R. L. (1996). Nonsense mutation in the human growth hormone-releasing hormone receptor causes growth failure analogous to the little (lit) mouse. *Nat. Genet.* **12**, 88-90. doi:10.1038/ng0196-88

Warmerdam, D. O., Alonso-de Vega, I., Wiegant, W. W., van den Broek, B., Rother, M. B., Wolthuis, R. M. F., Freire, R., van Attikum, H., Medema, R. H. and Smits, V. A. J. (2020). PHF6 promotes non-homologous end joining and G2 checkpoint recovery. *EMBO Rep.* **21**, e48460. doi:10.15252/embr.201948460

Watanabe, S., Tsunematsu, Y. and Fujimoto, J. (1988). Leukaemia in patients treated with growth hormone. *Lancet* **331**, 1159-1160. doi:10.1016/S0140-6736(88)91968-X

Watanabe, S., Mizuno, S., Oshima, L.-H., Tsunematsu, Y., Fujimoto, J. and Komiyama, A. (1993). Leukemia and other malignancies among GH users. *J. Pediatr. Endocrinol.* **6**, 99-108. doi:10.1515/JPEM.1993.6.1.99

Weber, F. T., Frias, J. L., Julius, R. L. and Felman, A. H. (1978). Primary hypogonadism in the Borjeson-Forssman-Lehmann syndrome. *J. Med. Genet.* **15**, 63-66. doi:10.1136/jmg.15.1.63

Webster, E., Cho, M. T., Alexander, N., Desai, S., Naidu, S., Bekheirnia, M. R., Lewis, A., Retterer, K., Juusola, J. and Chung, W. K. (2016). De novo PHIP-predicted deleterious variants are associated with developmental delay, intellectual disability, obesity, and dysmorphic features. *Cold Spring Harb. Mol. Case Stud.* **2**, a001172. doi:10.1101/mcs.a001172

Wendorff, A. A., Quinn, S. A., Rashkovan, M., Madubata, C. J., Ambesi-Impiombato, A., Litzow, M. R., Tallman, M. S., Paietta, E., Paganin, M., Basso, G. et al. (2019). Phf6 loss enhances HSC self-renewal driving tumor initiation and leukemia stem cell activity in T-ALL. *Cancer Discov.* **9**, 436-451. doi:10.1158/2159-8290.CD-18-1005

Wit, J. M., Oostdijk, W., Losekoot, M., van Duyvenvoorde, H. A., Ruivenkamp, C. A. and Kant, S. G. (2016). Mechanisms in endocrinology: novel genetic causes of short stature. *Eur. J. Endocrinol.* **174**, R145-R173. doi:10.1530/EJE-15-0937

Zhang, X., Fan, Y., Liu, X., Ang Zhu, M., Sun, Y., Yan, H., He, Y., Ye, X., Gu, X. and Yu, Y. (2019). A novel nonsense mutation of PHF6 in a female with extended phenotypes of Borjeson-Forssman-Lehmann syndrome. *J. Clin. Res. Pediatr. Endocrinol.* **11**, 419-425. doi:10.4274/jcrpe.galenos.2019.2018.0220

Zhou, Y., Xu, B. C., Maheshwari, H. G., He, L., Reed, M., Lozykowski, M., Okada, S., Cataldo, L., Coschigamo, K., Wagner, T. E. et al. (1997). A mammalian model for Laron syndrome produced by targeted disruption of the mouse growth hormone receptor/binding protein gene (the Laron mouse). *Proc. Natl. Acad. Sci. USA* **94**, 13215-13220. doi:10.1073/pnas.94.24.13215

Zweier, C., Kraus, C., Brueton, L., Cole, T., Degenhardt, F., Engels, H., Gillessen-Kaesbach, G., Graul-Neumann, L., Horn, D., Hoyer, J. et al. (2013). A new face of Borjeson-Forssman-Lehmann syndrome? De novo mutations in PHF6 in seven females with a distinct phenotype. *J. Med. Genet.* **50**, 838-847. doi:10.1136/jmedgenet-2013-101918